J Electr Eng Technol.2015; 10(4): 1480-1491
http://dx.doi.org/10.5370/JEET.2015.10.4.1480

ISSN(Print) 1975-0102
ISSN(Online) 2093-7423

# A New Approach to Short-term Price Forecast Strategy with an Artificial Neural Network Approach: Application to the Nord Pool

**Mun-Kyeom Kim†**

**Abstract** – In new deregulated electricity market, short-term price forecasting is key information for all market players. A better forecast of market-clearing price (MCP) helps market participants to strategically set up their bidding strategies for energy markets in the short-term. This paper presents a new prediction strategy to improve the need for more accurate short-term price forecasting tool at spot market using an artificial neural networks (ANNs). To build the forecasting ANN model, a three-layered feedforward neural network trained by the improved Levenberg-marquardt (LM) algorithm is used to forecast the locational marginal prices (LMPs). To accurately predict LMPs, actual power generation and load are considered as the input sets, and then the difference is used to predict price differences in the spot market. The proposed ANN model generalizes the relationship between the LMP in each area and the unconstrained MCP during the same period of time. The LMP calculation is iterated so that the capacity between the areas is maximized and the mechanism itself helps to relieve grid congestion. The addition of flow between the areas gives the LMPs a new equilibrium point, which is balanced when taking the transfer capacity into account, LMP forecasting is then possible. The proposed forecasting strategy is tested on the spot market of the Nord Pool. The validity, the efficiency, and effectiveness of the proposed approach are shown by comparing with time-series models

**Keywords**: Short-term forecasting, Locational marginal price, Artificial neural network, Levenberg-marquardt algorithm, Nord pool

## Nomenclature

| | |
|---|---|
| $N$ | forecast horizon |
| $D$ | demand in the spot market (MW) |
| $V$ | volume difference between the power generation and load |
| $P_{MCP}$ | market-clearing price (MCP) |
| $P_{LMP}$ | locational marginal price (LMP) |
| $P_{MCP_t}$ , $P_{LMP_t}$ | MCP and LMP at $t$-hour in the spot market, respectively |
| $P_{LMP_t}^{Act}$ , $P_{LMP_t}^{For}$ | actual and forecasted LMPs at $t$-hour, respectively |
| $\Delta P$ | price difference between bidding areas |
| $\Delta P_{LMP_t}$ | LMP difference for each of bidding area at $t$-hour in the spot market. |
| $P_{LMP_t}^{Act\_Ave}$ | average actual LMPs of the forecasting period |
| $L^{actual}$ | actual system load (MW) |
| $G^{actual}$ | actual generation volume (MW), |
| $G_{R\_(t-i)}^{actual}$ | actual power generation $i$ hours ago in the $R$ bidding area |
| $L_{R\_(t-i)}^{actual}$ | actual system load $i$ hours ago in the $R$ bidding area |
| $\omega$ | scalar parameter |
| $\pi 1$, $\pi 2$ | multiplication factor and division factor, respectively |
| $E(\alpha)$ | error vector |
| $J(\alpha)$ | Jacobian matrix |
| $\nabla f(\alpha)$ | gradient vector |
| $\nabla^2 f(\alpha)$ | Hessian matrix |

† Corresponding Author: Dept. of Energy System Engineering, Chung-Ang University, Korea. (mkim@cau.ac.kr)
Received: June 3, 2014; Accepted: March 30, 2015

## 1. Introduction

In restructuring the electric power industry, the price of electricity has become a fundamental input to any energy company's decision-making. With this global reformation, the industry is moving towards privatization and liberalization [1]. The primary goal of energy deregulation is to encourage not only the competition between market participants, but also the development of a more reliable energy-supply mechanism with lower costs. A producer needs to forecast electricity prices to determine its bidding strategy in the power market and to optimally schedule its electric energy resources, such as hydro and thermal resources. Each entity predicts market prices and develops strategies, based on accurately forecast market prices with other information on opportunities, to create profits before participating in the electricity market. Consumers also need price forecasts for the same reasons as producers [2]. If the electricity market price can be predicted properly, market participants can reduce the risks of under/overestimating revenue from the generators for the power companies and maximizes their outcomes further. As a result, proper electricity price forecasting can help in building cost-effective risk management plans for the companies participating in the electricity market.

The primary role of a market price is to establish an equilibrium between supply and demand. This means that prices rise or fall in the short term until supply and demand become equal. Generally, electrical energy is traded as a commodity; however, electricity is an extraordinary product, because its price has a complex signal due to its non-linear, non stationary, and time-variant behavior [3]. In the current deregulated scenario, load forecasting has reached an advanced stage of development [4-8], while price-forecasting techniques, which are being applied, are still in the early stages of maturity. In actual electricity markets, daily load curves have similar load patterns, whereas price curves exhibit considerably richer structures because their movement shows great volatility [9]. Even accurate load forecasts cannot guarantee profits, and the potential increasing risk due to trading is considerable because of the extreme volatility of electricity prices. At the same time, market participants usually have limited and uncertain information for price prediction.

Electricity price forecasting is generally divided into long-term and short-term, depending on the forecasting period [10]. In particular, short-term electricity price forecasting is important due to its profit function; all participants need to make reasonable decisions and to maximize utility profits during market business activities. This can be achieved by considering changes with time scales ranging from a few minutes to about one week, while assuming other fixed middle- and long-term factors. Additionally, the most basic pricing concept in the power market is the market-clearing price (MCP) [11-13]. In an unconstrained market-clearing process, generator companies are dispatched based on their bidding prices. When there are no transmission constraints, locational marginal price (LMP) is the same at any point in the entire system, and is equal to the MCP. However, when there is congestion, transmission line constraints are considered to balance supply and demand at each point. The system generation dispatch then differs from the least bidding price dispatch, and LMPs can vary throughout the transmission system. In this situation, the price in a constrained area is higher than the unconstrained MCP.

Good LMP prediction is a difficult task because bidding strategies used by participants are complex, and various uncertainties interact in intricate ways. Moreover, a key aspect of LMPs is their volatility. Price volatility is crucial to calculate average annual prices and to derive bilateral contract prices for them. Obviously, a more accurate forecasting model can be helpful to generating companies in submitting accurate bids with low risk and, if necessary, to make good bilateral contracts [14]. In recent years, several methods have been used to predict prices in electricity markets. Stationary time-series models have been proposed, such as auto-regressive (AR) [15], dynamic regression and transfer function [16], and auto-regressive integrated moving-average (ARIMA) techniques [17]. The wavelet-ARIMA technique [18] and the generalized auto-regressive conditional heteroskedastic (GARCH) models [19-20], which consider the moments of a time series as variants, have been used to forecast electricity prices in deregulated electricity markets. Unfortunately, most time-series models are linear prediction models, tracing patterns in historic input data, whereas electricity prices represent a non-linear function of the input features. Thus, the behavior of a price signal may not be completely captured by any time-series technique.

To solve these problems, another kind of forecasting method, based on intelligence techniques, and especially artificial neural networks (ANNs), has been proposed by researchers [21-29]. ANNs are simple, but powerful and flexible tools for analyzing factors that could impact electricity prices. From a mathematical point of view, an ANN is a universal functional approximator, based on the functioning of the human brain. Theoretically, it has been shown that, given an appropriate number of hidden units and enough computational resources, ANN can learn from experience and estimate any complex functional relationship. Moreover, ANNs are non-linear by nature, which means that they can not only correctly estimate non-linear functions, but also extract non-linear elements from data and are able to solve problems where the input output relationship is neither well defined nor readily computable, because ANNs are data driven. The powerful ability to simulate dynamic, uncertain, and nonlinear problems makes ANNs suitable for predictions in electrical power systems. In [30], combination of similar days and neural network techniques were proposed for LMP prediction. However, traditional training algorithms such as back-propagation may drive the network to get trapped in local minima and slow speed of convergence. In [31], the recurrent neural network was also developed for forecasting the LMPs to speed up the offline training process. Some other researchers proposed specific methods for price spike forecasting in [32-33]. Despite the research performed in this area, there is a continuing need for more accurate and robust price forecast methods for large-scale power systems.

This paper proposes a new forecasting strategy to predict short-term prices in the spot market. The whole proposed forecasting strategy is examined using the Nord Pool, one of the most successful electrical power markets in the world. The main contributions of this paper can be summarized as follows:

- A neural network approach, including the LM algorithm to train a three-layered feed forward neural network that improves ANN training, in terms of error and consumption time, is developed to forecast short-term electricity prices.

- To accurately predict LMPs, the most effective input features based on actual power generation and load are used for more accurate LMP forecasting, and these differences are applied to predict price differences in the spot market.
- By analyzing the causes of price differences, the LMP calculation is iterated so that the available trading capacity between the areas is used to the maximum during every hour of operation. After the addition of flow between the areas, the LMP forecasting is obtained.
- The proposed approach is compared with a time-series model using a realistic case study based on electricity data from the Nord Pool.
- The proposed forecasting strategy provides reasonable forecasts for LMPs. In particular, it shows high accuracy in forecasting LMPs during peak times. This aspect gives effective information to market participants and helps them to make sound, profitable decisions.

This paper is organized as follows: Section 2 provides the neural network structure to forecast electricity prices. Section 3 presents the forecasting strategy to evaluate the LMPs. Section 4 provides the numerical results from a real-world case study based on data from the Nord Pool. Finally, concluding remarks are given in Section 5.

## 2. Forecasting with an ANN Model

ANN is a simple but powerful tool that can be trained by adopting a forecasting process. The advantages of the ANN mainly lie in self-training ability [34]. The ANN builds its structure by learning patterns from repeated data and, through the process, the completed structure have the ability to generalize. This ability implies that the acquired patterns of input / output relations of the ANN and the ANN itself are capable of producing comparatively correct output from an inexperienced input without requiring any further process.

An ANN is composed of three different layers – input, hidden, and output layers – each of which consists of a certain number of neurons and one or more individual nodes or processing elements. The main idea with an ANN is that inputs, or dependent variables, get filtered through one or more hidden layers before they reach the output variable. The number of input variables necessary to predict the desired output variables determines the number of input nodes. The outputs of the hidden layer translate the input into the output layer of neurons, and the optimum number of hidden nodes and hidden layers are dependent on the complexity of the modeling problem. Thus, the neural network considered is fully connected in the sense that every node belonging to each layer is connected to every other node belonging to the adjacent forward layer. In ANNs, the most popular and successful model is the multi-layer feed-forward neural network (MLNN). In particular, a three-layer feed-forward neural network is suited for forecasting, implementing non-linear hyperbolic-tangent sigmoid activation functions for the hidden layer and pure linear transfer functions for the output layer.

Forecasting with neural networks consists of two stages: the training stage and the learning stage. In the training stage, a training set is used for construction of the neural network. This typically requires a training set of historical data, containing both inputs and the corresponding desired outputs. During training, it is identified a suitable training set with patterns of input and corresponding output pairs, and is trained the ANN for price forecasting. In the learning stage, learning entails an optimization process – the minimization of some error measure between the output produced and the desired output. The learning algorithm iteratively adjusts the values of connection weights within the ANN structure. Then, the knowledge gained through the learning process is tested by applying new data. The data series is called the testing set, which is used for measuring the predictive ability of the model.

For a large-scale system, it is more desirable to attain the desired accuracy with a simpler ANN structure – i.e., fewer nodes – because this can reduce training time, improve network generalization, and prevent over-fitting. The back-propagation algorithm is widely recognized as a powerful tool for training of MLNNs. However, because it applies the steepest descent method to update the weights, it suffers from a slow convergence rate and often yields suboptimal solutions. The Levenberg – Marquardt (LM) algorithm used in this study is one of the most efficient training mechanisms for prediction tasks because it provides high degrees of robustness and generalization [35]. The LM algorithm trains a neural network 10 – 100 times faster than the usual gradient-descent back-propagation method. This algorithm is an approximation of Newton's method, and it computes an approximate Hessian matrix. The quasi-Newton technique for minimizing a function $f(\alpha)$ with respect to the parameter vector α is given by:

$$\Delta\alpha = -\left[\nabla^2 f(\alpha)\right]^{-1} \nabla f(\alpha) \tag{1}$$

Assuming that $f(\alpha)$ is the sum of squares function, given by

$$f(\alpha) = \sum_{i=1}^{N} E_i^2(\alpha) \tag{2}$$

then it can be shown that:

$$\nabla f(\alpha) = J^T(\alpha)E(\alpha) \tag{3}$$

$$\nabla^2 f(\alpha) = J^T(\alpha)J(\alpha) + U(\alpha) \tag{4}$$

Here, $J(\alpha)$ is given by

$$J(\alpha)=\begin{bmatrix} \frac{\partial E_1(\alpha)}{\partial \alpha_1} & \frac{\partial E_1(\alpha)}{\partial \alpha_2} & \cdots & \frac{\partial E_1(\alpha)}{\partial \alpha_n} \\ \frac{\partial E_2(\alpha)}{\partial \alpha_1} & \frac{\partial E_2(\alpha)}{\partial \alpha_2} & \cdots & \frac{\partial E_2(\alpha)}{\partial \alpha_n} \\ \vdots & \vdots & \ddots & \vdots \\ \frac{\partial E_N(\alpha)}{\partial \alpha_1} & \frac{\partial E_N(\alpha)}{\partial \alpha_2} & \cdots & \frac{\partial E_N(\alpha)}{\partial \alpha_n} \end{bmatrix} \tag{5}$$

where $U(\alpha)$ is given by

$$U(\alpha)=\sum_{I=1}^{n} E_i(\alpha)\nabla^2 E_i(\alpha) \tag{6}$$

Assuming that $U(\alpha)\approx 0$, the Hessian matrix is given by

$$\nabla^2 U(\alpha)=2J^T(\alpha)J(\alpha) \tag{7}$$

and the update (1) becomes:

$$\Delta\alpha=-\left[J^T(\alpha)J(\alpha)\right]^{-1}J^T(\alpha)E(\alpha) \tag{8}$$

The LM algorithm for the Gauss–Newton method is defined as:

$$\Delta\alpha=-\left[J^T(\alpha)J(\alpha)+\omega I\right]^{-1}J^T(\alpha)E(\alpha) \tag{9}$$

where parameter $\omega$ is conveniently modified during the algorithm iterations. Note that when $\omega$ is large, the LM algorithm becomes steepest descent, while for small $\omega$, the algorithm becomes Gauss-Newton, which should provide faster convergence. An update of $\omega$ that is too big or too small will cause the neural network to take longer to train. The disadvantage is similar with the learning rate in the standard back propagation algorithm. An appropriate update of $\omega$ is more efficient for convergence. The rule for the adjustment of $\omega$ is as follows.

$$\omega(t)=\begin{cases} \omega(t-1)\times\pi_1\,, & if \quad E(t)>E(t-1) \\ \omega(t)=\omega(t)\,, & if \quad E(t)=E(t-1) \\ \dfrac{\omega(t-1)}{\pi_2}\,, & if \quad E(t)<E(t-1) \end{cases} \tag{10}$$

In traditional LM algorithm the parameter $\omega$ is multiplied by some factor ($\pi$) whenever a step would result in an increased C($x$) (a cost function which should be minimized). When step reduces C($x$), $\omega$ is divided by $\pi$. It is noted that when $\omega$ is large, convergence is improved, but the learning time is increased; while for small $\omega$, learning time is reduced, but error goal is also decreased. To get better results and less time consumption, the $\omega$ multiplication factor ($\pi$1) is often set larger than the $\omega$ division factor ($\pi$2). In the algorithm, the rate of change in $\omega$ is exponential. In this paper, increasing rate ($\pi$1) and decreasing rate ($\pi$2) of $\omega$ with using the heuristic method [36] is used to improve the traditional LM algorithm. The modification on LM algorithm provides the best performance in terms of convergence time, optimum network structure, and recognition performance.

## 3. Proposed Price Forecast Strategy

### 3.1 Input factor selection

The price of electricity is influenced by many relevant factors, such as electrical load, available generation, weather conditions, time indicators, generation outages, transmission network information, and bidding strategies of market participants. Some of these factors are more important than others. In fact, the factors that really impact the price are applied to be very limited, typically, just the electrical load. In this paper, two types of electrical load are considered when predicting electricity prices. One is demand in the spot market and the other is the actual load in the entire power system. The effect of the temperature and other weather-related factors can be incorporated into electricity load. Another factor that drives the price is the hour of the day; however, the impact is also reflected in electricity load [15]. The unit outage information, although significant, was not considered in the study because it is typically proprietary and not available to all market participants in real time. Each Nordic country is separated into several bidding areas with various power generation sources and available transmission capacity may vary, but all of transmission network information are not recorded in the SCADA systems. Moreover, there are some factors, such as bidding strategies and unethical competitive behavior that are not easily represented in mathematical form.

### 3.2 Overview of nord pool

Nord Pool is the first multinational electricity market in the world, and is evaluated as successful a market, according to industry representatives and electricity market analysis. In the Nord Pool, Elspot is a spot auction-based day-ahead energy market in which market participants submit offers to sell or bids to buy physical electricity for delivery in each hour the next day. Nord Pool organizes the bids and the power flows over the interconnectors, and is coordinated by the system operator who ensures a secured, economical and efficient operation as well as determining all LMP according to voluntary bids and bilateral transactions.

Electricity is generated from different energy sources in the Nordic countries. Hydropower covers half of the power needs in the Nordic system. In Norway, almost all power is supplied by hydropower, while Sweden has a mix of conventional thermal power, nuclear power, and hydropower, which is about 50% of total power capacity. Thus, Norway and Sweden jointly contribute a high proportion of hydroelectric power to the Nord Pool. Denmark uses mainly thermal power, but wind power is becoming increasingly important. Finland has a similar mix of generation as Sweden, but with higher shares of thermal and nuclear power than hydropower.

### 3.3 Relationship between market structure and pricing mechanism

Price evaluation differs across market structures and no single available model has been applied across a broad spectrum of market data [26]. There is no systematic evidence of one model consistently out-performing others. This may be due to the short history of electricity markets and the substantial differences in price developments that exist in electricity markets. Moreover, LMPs depend on market player behavior because the multi-settlement system provides market participants with the ability to develop complex strategies.

In an unconstrained market-clearing process, the most basic pricing concept is the MCP. Fig. 1 illustrates that the MCP is determined based on hourly bids from both supply- and demand-side participants for the trading of prompt physically delivered electricity. Each order from market participants in the spot market specifies the volume in MWh/h that a participant is willing to buy or sell at specific price levels. Whenever the power flow between the bidding areas is within the limits set by the system operator, the MCP is the only price for that specific hour throughout the entire system. In this situation, the MCP must be directly influenced by demand in the spot market and is formulated as follows:

$$P_{MCP} = F(D) \tag{11}$$

However, congestion can cause differences in prices among bidding areas. When the power transfer between bidding areas exceeds the trading capacity and transmission

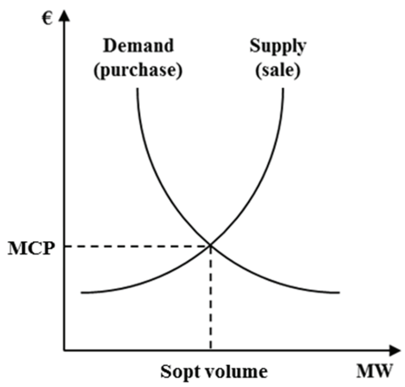


**Fig. 1.** MCP in the nord pool

congestion is predicted, the LMPs could be employed. LMP is defined as the price of lowest-cost resources available to meet the load, subject to delivery constraints of the physical network. LMP is an efficient way of pricing energy supply when transmission constraints exist. In the end, load differences between several areas change the LMPs, and then the electricity load is not the demand in the spot market but the actual load of the entire power system.

$$P_{LMP} = F(L^{actual}) \tag{12}$$

Eq. (12) represents the LMPs as a function of load in the entire power system, but it does not fully reflect the LMP signal because the transfer capacity also influences the transmission congestion.

### 3.4 LMP forecasting

Whenever congestion takes place in transmission grids, each Nordic country is separated into several bidding areas. Available transmission capacity may vary, and thus LMPs are established for each transmission-constrained area, as shown in Fig. 2. The LMPs are published within two hours of the Elspot market closing. A lower price in the surplus area will lead to greater purchases and fewer sales, which can provide a parallel shift in the demand curve. However, by increasing the price in the deficit area, the area participants sell more and purchase less, and the sale can provide a parallel shift in the supply curve. Here, PL and PH represent the low and high prices when there is full utilization of trading capacity. PCap=0 is a price in an area with an isolated price calculation. The LMP calculation is iterated so that the available trading capacity between the high price and the low price area is used to the maximum during every hour of operation, to ensure that power flows from the low-price area towards the high-price area. Accordingly, the LMPs in the surplus and deficit areas are the new equilibrium points following the addition of power flow between the areas of purchase and sale. In this situation, the LMPs are relatively low in the surplus area (PL) and relatively high in the deficit area (PH).

The transfer capacity is the maximum amount of energy that can flow from one bidding area to another [37]. The system operator determines the trading capacities for each hour of the day and receives income from market splitting. To accurately predict the LMPs, a volume corresponding to the trading capacity on the constrained connection should be considered at a relatively low price in the surplus area and a relatively high price in the deficit area. Price differences between bidding areas occur when the surplus volume at the MCP in one or more bidding areas is greater than the total export capacity from these areas. Thus, the total export capacity for each of these areas can be used for analyzing the cause of price differences,

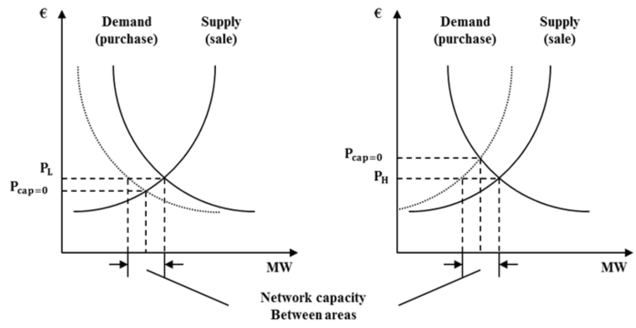


(a) Surplus area (b) Deficit area

**Fig. 2.** LMPs in the nord pool

$$\Delta P = F(G^{actual} - L^{actual}) = F(V) \tag{13}$$

The forecast result varies depending on which and how the input data are used. In this work, the actual power generation and load are predicted as the input set. First, to model the trends in the power generation signal, the actual generating volume in the same hour over previous periods are considered as input features,

$$\begin{aligned} G^{actual}_{R\_(t-i)} = F(&G^{actual}_{R\_(t-1)}, G^{actual}_{R\_(t-2)}, G^{actual}_{R\_(t-3)}, G^{actual}_{R\_(t-4)}, \mathrm{a} \\ &G^{actual}_{R\_(t-23)}, G^{actual}_{R\_(t-24)}, G^{actual}_{R\_(t-25)}, G^{actual}_{R\_(t-47)}, \\ &G^{actual}_{R\_(t-48)}, G^{actual}_{R\_(t-49)}, G^{actual}_{R\_(t-167)}, G^{actual}_{R\_(t-168)}, \\ &G^{actual}_{R\_(t-169)}, G^{actual}_{R\_(t-335)}, G^{actual}_{R\_(t-336)}, G^{actual}_{R\_(t-337)}, \\ &G^{actual}_{R\_(t-503)}, G^{actual}_{R\_(t-504)}, G^{actual}_{R\_(t-505)}, G^{actual}_{R\_(t-671)}, \\ &G^{actual}_{R\_(t-672)}, G^{actual}_{R\_(t-673)}) \end{aligned} \tag{14}$$

Typically, the shapes of the price profiles present seasonality characteristics, usually in terms of daily and weekly cycles. The price profile is modified from day-to-day and week-to-week to reflect changes in the electricity market behavior. Instead of single similar-day power generation, the forecast can be a linear combination or a regression procedure that can include several similar days. For daily seasonality, in addition to $G^{actual}_{R\_(t-24)}$ (actual generating volume of 24 h ago in the R bidding area), $G^{actual}_{R\_(t-23)}$ and $G^{actual}_{R\_(t-25)}$ can also be considered, and similarly for other periods. In (14), the first four terms consist of information about the trends in the signal. The next six terms contain information about daily seasonality (up to 2 days ago), while the latter twelve terms are related to weekly seasonality (1-4 weeks ago).

Similarly, the actual load during previous hours is considered due to its high correlation with the next hourly load. The following set of input features can be considered for actual load prediction:

$$\begin{aligned} L^{actual}_{R\_(t-i)} = F(&L^{actual}_{R\_(t-1)}, L^{actual}_{R\_(t-2)}, L^{actual}_{R\_(t-3)}, L^{actual}_{R\_(t-4)}, \\ &L^{actual}_{R\_(t-23)}, L^{actual}_{R\_(t-24)}, L^{actual}_{R\_(t-25)}, L^{actual}_{R\_(t-47)}, \\ &L^{actual}_{R\_(t-48)}, L^{actual}_{R\_(t-49)}, L^{actual}_{R\_(t-167)}, L^{actual}_{R\_(t-168)}, \\ &L^{actual}_{R\_(t-169)}, L^{actual}_{R\_(t-335)}, L^{actual}_{R\_(t-336)}, L^{actual}_{R\_(t-337)}, \\ &L^{actual}_{R\_(t-503)}, L^{actual}_{R\_(t-504)}, L^{actual}_{R\_(t-505)}, L^{actual}_{R\_(t-671)}, \\ &L^{actual}_{R\_(t-672)}, L^{actual}_{R\_(t-673)}) \end{aligned} \tag{15}$$

The selection of similar days is part of the training in the ANN. The training data are classified as weekdays from Monday to Friday and weekends as Saturday and Sunday. For example, eight similar days are selected for training to predict the price on Monday or Sunday etc. One day is taken from the similar days as test data. A similar day is characterized as follows. A Monday is similar to the Monday of the previous week and the same rule applies for Saturdays and Sundays; analogously, a Tuesday is similar to the Monday of the same week, and the same rule applies for Wednesdays, Thursdays and Fridays [30].

In our study, these differences between actual power generation and load are used to predict the price differences in the spot market. The proposed ANN model generalizes the relationship between the respective LMPs and the MCP during the same period of time. Then, the LMP is calculated as follows:

$$P_{LMP_t} = P_{MCP_t} + \Delta P_{LMP_t} \tag{16}$$

The LMP calculation is iterated so that the capacity between areas is used to the maximum; this mechanism itself actually helps to relieve grid congestion. After that, and the addition of flow between the areas, the LMP is determined at the new equilibrium point, which is balanced taking the transfer capacity into account.

## 4. Numerical Results

As in any research area, it is vital to allow the reproduction of one's results in price forecasting. The only way of doing that is the use of public-domain data sets. The proposed forecasting approach was used to predict LMPs in the Nord Pool using real market data, obtained from [38]. The Nord Pool maintains the confidentiality of the bid information of each market participant confidential; however, the market price and the aggregate volumes are publicly available. All price data are in Euros. To satisfy performance, the proposed approach was compared with time series models, ARIMA [17] and GARCH [20]. Detail of this time series models can be found in the Appendix.

For each Nordic country, the system operators decide which bidding areas the country is divided into. The bidding areas are denoted by an alphanumeric code, such as NO1, NO2, NO3, DK1, DK2, SE, and FI. The Norwegian system operator defines the fixed bidding areas in Norway, according to its information on the likely pattern of flows in the system for a certain period of time. The number of Norwegian bidding areas can vary; in this paper, three bidding areas are defined as NO1, NO2, and NO3. When necessary, additional price areas may be used. Western Denmark (DK1) and eastern Denmark (DK2) are always treated as different bidding areas, and Sweden (SE) and Finland (FI) constitute one bidding area each.

### 4.1 Simulation

The three-layered feed-forward neural network with the LM structure employed in the study used the "newff" function implemented in MATLAB [39]. Transfer functions were used for the hidden and output layers. At the training stage, various numbers of units in the hidden layer were tested. The number of neurons in the hidden layer varies for different applications and usually depends on the size of the training set and the number of input variables. Fortunately, using MATLAB, it was a straightforward task to compare the impact of the number of hidden-layer neurons on the performance of the ANN. When the various numbers of neurons in the hidden layer were tested, the best results were produced with five hidden. The output layer had one unit, which was set to output the LMPs. Besides, very large training sets should not be used to avoid overtraining during the learning process. On the other hand, if the selected training period is very short, then the ANN cannot derive all of the functional relationships in the electricity prices due to the small number of training samples.

In this paper, the training set was defined as the three-month period from April 13 to July 12, 2009, and the testing set started from July 15, 2009, after the training period, because the Elspot closes at 12.00 am and there are at least 12 hours, and at most 36 hours, between the time of trade and the time of delivery. Thus, our forecasts is made on an hourly basis for 2 days during the forecast period, and this cycle is repeated until the LMPs of the whole forecast horizon are predicted. Additionally, the training data includes 91×24=2,184 learning patterns. After the tests were conducted through the different parameters, the training parameters were as follows: $\pi 1 = 3$ and $\pi 2 = 1.12$. All the simulations were implemented with MATLAB on an Intel Xeon processor E5620 with eight quad-core processors having a clock speed of 2.4 GHz and 12 GB of RAM memory.

### 4.2 Evaluating the forecasting error

Forecasting error is the main concern for system operator; a lower error indicates a better result. This accuracy is computed as a function of the actual prices that occurred. Since a set of non-stationary data is studied, a statistical analysis is more reasonable. To evaluate the accuracy in forecasting electricity prices, four different criterions are used: the mean absolute error (MAE) criterion, the root mean square error (RMSE) criterion, the mean absolute percentage error (MAPE) criterion, and the error variance ($\sigma^2$). They are expressed in the following:

$$\mathrm{MAE} = \frac{1}{N}\sum_{t=1}^{N}\left|P_{LMP_t}^{Act} - P_{LMP_t}^{For}\right| \tag{17}$$

$$\mathrm{RMSE} = \sqrt{\frac{1}{N}\sum_{t=1}^{N}\left(P_{LMP_t}^{Act} - P_{LMP_t}^{For}\right)^2} \tag{18}$$

$$\mathrm{MAPE} = \frac{1}{N}\sum_{t=1}^{N}\frac{\left|P_{LMP_t}^{Act} - P_{LMP_t}^{For}\right|}{P_{LMP_t}^{Act\_Ave}}\times 100 \tag{19}$$

$$\sigma^2 = \frac{1}{N}\sum_{t=1}^{N}\left[\frac{\left|P_{LMP_t}^{Act} - P_{LMP_t}^{For}\right|}{P_{LMP_t}^{Act\_Ave}} - \mathrm{MAPE}\right]^2 \tag{20}$$

where:

$$P_{LMP_t}^{Act\_Ave} = \frac{1}{N}\sum_{t=1}^{N}P_{LMP_t}^{Act} \tag{21}$$

The reason for considering average LMPs in Eq. (21) is that if the actual value is small, this will contribute large term in MAPE even if the difference between actual and forecasted values is small. In addition, if the forecasted value is small and actual value is large, and then absolute percentage error will be close to 100%. Furthermore, the LMP can rise to tens or even hundreds of times of its normal value at particular hours. It may drop to zero or even to negative at other hours. Hence, the average LMP is used in Eq. (21) to avoid the adverse effects of prices close to zero.

### 4.3 Forecasting results of LMP

When using the ANN for price forecasting, first, parameters that would fit the neural network with a LM structure, based on historical data are identified, and then future prices are predicted. In the Nord Pool, the MCP is forecast from the input set of demand in the spot market, and is expressed as a function:

$$\begin{aligned} P_{MCP_t} = F(&D_{\mathrm{NO1\_t}}, D_{\mathrm{NO2\_t}}, D_{\mathrm{NO3\_t}}, \\ &D_{\mathrm{DK1\_t}}, D_{\mathrm{DK2\_t}}, D_{\mathrm{SE\_t}}, D_{\mathrm{FI\_t}}) \end{aligned} \tag{22}$$

Table 1 shows the results of actual and forecast MCPs for the test period, respectively. It can be seen that the proposed approach indicates good performance in MCP forecasting. Notably, accurate price predictions were also obtained during peak hours in the Nordic spot market.

For forecasting the LMP, actual power generation and load were considered as input sets, and then these volume differences were used to predict the price differences. From

(13) – (16), the following price difference in the Nordic area can be obtained readily:

$$\Delta P_{LMP_t} = F(V_{\mathrm{NO1\_t}}, V_{\mathrm{NO2\_t}}, V_{\mathrm{NO3\_t}}, V_{\mathrm{DK1\_t}}, V_{\mathrm{DK2\_t}}, V_{\mathrm{SE\_t}}, V_{\mathrm{FI\_t}}) \tag{23}$$

The relationships between each LMP and the MCP during the same period of time are generalized using the proposed ANN model, and then LMP forecasting was obtained as illustrated in Table 2. The results obtained indicate good performance for the LMP forecasting capabilities during the test period. It is generally observed that the peak, because of its high volatility and price spikes, is the most difficult feature to predict. However, especially for peak hours, accurate predictions were obtained using the proposed forecasting strategy. This gives effective information for market participants and helps them make sound, profitable decisions, because of the high power-trading volume at the time of peak demand.

As shown in Table 2, a hydropower area like NO1, NO2, and NO3 has the LMP that is lower than the MCP. Hydropower is easily regulated, and can show substantial differences during the day. For this reason, the transmission requirements can vary greatly. In the end, LMPs depend on inflows to reservoirs. There can be daily and hourly patterns, with less price variations in hydropower-dominant areas due to the high degree of controllability. On the other hand, the LMPs for DK1, DK2, and FI are above the MCP. FI has a similar mix of generation methods as Sweden, but with a higher share of thermal and nuclear power instead of hydropower. DK1 and DK2 have mainly thermal power generation, with an increasing share of wind power. This has implications for power trading between the Nordic countries. Due to higher price volatility in DK1, and especially in FI, there were slight differences between the forecast LMP and actual LMP during the test period.

Moreover, comparing SE and FI, the LMPs are of vital importance for the efficient use of hydropower in the mixed hydrothermal Nordic system.

To assess the prediction accuracy of the proposed approach, Fig. 3 and Fig. 4 show hourly MAE and MAPE values for test periods in the Nordic area, respectively. Table 3 also summarizes different statistical measures for

**Table 1.** MCP forecasting in the Nord Pool

| Hour | Forecasted MCPs (EUR/MWh) | Actual MCPs (EUR/MWh) |
|---|---|---|
| 00–01 | 32.89 | 31.07 |
| 01–02 | 30.65 | 29.7 |
| 02–03 | 29.47 | 28.12 |
| 03–04 | 29.22 | 27.48 |
| 04–05 | 28.29 | 27.85 |
| 05–06 | 30.77 | 30.7 |
| 06–07 | 33.71 | 33.13 |
| 07–08 | 35.11 | 34.31 |
| 08–09 | 35.93 | 35.72 |
| 09–10 | 36.55 | 36.37 |
| 10–11 | 36.34 | 37.34 |
| 11–12 | 36.27 | 38.45 |
| 12–13 | 36.49 | 38.6 |
| 13–14 | 35.93 | 37.3 |
| 14–15 | 35.68 | 36.93 |
| 15–16 | 36.09 | 35.76 |
| 16–17 | 35.12 | 34.52 |
| 17–18 | 35.36 | 34.48 |
| 18–19 | 35.73 | 34.34 |
| 19–20 | 35.48 | 33.99 |
| 20–21 | 34.01 | 33.94 |
| 21–22 | 34.35 | 34.23 |
| 22–23 | 33.61 | 33.61 |
| 23–24 | 32.54 | 31.5 |

**Table 2.** Results of LMP for the test periods in the Nord Pool

| Hour | Forecasted LMP (EUR/MWh) | | | | | | | Actual LMP (EUR/MWh) | | | | | | |
|---|---|---|---|---|---|---|---|---|---|---|---|---|---|---|
| | NO1 | NO2 | NO3 | DK1 | DK2 | SE | FI | NO1 | NO2 | NO3 | DK1 | DK2 | SE | FI |
| 00–01 | 33.01 | 32.54 | 32.82 | 34.69 | 33.36 | 32.40 | 32.46 | 31.49 | 33.05 | 31.49 | 31.49 | 31.49 | 31.49 | 31.49 |
| 01–02 | 30.67 | 30.71 | 30.76 | 31.70 | 30.53 | 29.91 | 29.96 | 29.15 | 32.77 | 29.15 | 29.15 | 29.15 | 29.15 | 29.15 |
| 02–03 | 29.47 | 29.68 | 29.64 | 29.94 | 29.23 | 28.95 | 28.98 | 26.98 | 32.64 | 26.98 | 26.98 | 26.98 | 26.98 | 26.98 |
| 03–04 | 29.06 | 29.75 | 29.51 | 29.28 | 29.06 | 28.96 | 28.97 | 25.75 | 32.62 | 25.75 | 25.75 | 25.75 | 25.75 | 25.75 |
| 04–05 | 28.04 | 29.09 | 28.71 | 27.96 | 27.84 | 27.90 | 27.90 | 26.49 | 32.14 | 26.49 | 26.49 | 26.49 | 26.49 | 26.49 |
| 05–06 | 30.72 | 31.16 | 31.05 | 30.77 | 30.26 | 30.23 | 30.25 | 29.71 | 32.10 | 31.81 | 29.71 | 31.81 | 31.81 | 31.81 |
| 06–07 | 33.99 | 32.58 | 33.33 | 37.07 | 35.07 | 33.41 | 33.49 | 32.29 | 33.15 | 33.15 | 29.10 | 33.15 | 33.15 | 42.45 |
| 07–08 | 33.92 | 35.10 | 35.43 | 39.57 | 39.55 | 38.67 | 38.64 | 32.83 | 33.48 | 33.48 | 41.80 | 38.61 | 38.61 | 46.15 |
| 08–09 | 34.18 | 35.42 | 35.89 | 45.6 | 44.81 | 40.76 | 40.76 | 33.44 | 33.77 | 33.77 | 41.11 | 41.11 | 41.11 | 50.92 |
| 09–10 | 34.87 | 36.19 | 36.60 | 44.82 | 44.57 | 41.17 | 41.16 | 33.64 | 33.83 | 33.83 | 40.83 | 40.83 | 40.83 | 51.54 |
| 10–11 | 34.81 | 35.95 | 36.38 | 44.17 | 43.75 | 40.63 | 40.63 | 33.99 | 34.01 | 34.01 | 42.32 | 42.32 | 42.32 | 44.66 |
| 11–12 | 34.63 | 35.91 | 36.34 | 44.53 | 44.03 | 40.86 | 40.85 | 33.87 | 34.23 | 34.23 | 44.26 | 44.26 | 44.26 | 48.55 |
| 12–13 | 35.07 | 36.09 | 36.52 | 43.63 | 43.34 | 40.45 | 40.45 | 33.94 | 34.21 | 34.21 | 43.97 | 43.97 | 43.97 | 47.11 |
| 13–14 | 34.80 | 35.54 | 35.95 | 41.76 | 41.50 | 39.14 | 39.14 | 33.79 | 34.20 | 34.20 | 42.79 | 42.79 | 42.79 | 42.79 |
| 14–15 | 34.80 | 35.33 | 35.73 | 40.20 | 39.99 | 38.27 | 38.27 | 33.59 | 34.15 | 34.15 | 41.56 | 41.56 | 41.56 | 41.56 |
| 15–16 | 35.41 | 35.79 | 36.19 | 39.29 | 39.30 | 38.22 | 38.23 | 33.48 | 33.97 | 33.97 | 39.32 | 39.97 | 39.97 | 39.97 |
| 16–17 | 35.04 | 34.45 | 35.01 | 37.69 | 36.71 | 35.81 | 35.84 | 33.58 | 33.80 | 33.80 | 37.41 | 37.41 | 37.41 | 37.41 |
| 17–18 | 35.50 | 34.59 | 35.19 | 38.00 | 36.41 | 35.53 | 35.57 | 33.50 | 33.83 | 33.83 | 37.36 | 37.36 | 37.36 | 37.36 |
| 18–19 | 35.52 | 35.02 | 35.56 | 39.31 | 38.22 | 36.69 | 36.73 | 33.44 | 33.73 | 33.73 | 37.41 | 37.41 | 37.41 | 38.59 |
| 19–20 | 36.02 | 33.95 | 34.96 | 39.13 | 36.34 | 34.64 | 34.74 | 33.25 | 33.71 | 33.71 | 35.43 | 35.43 | 35.43 | 39.01 |
| 20–21 | 34.49 | 32.47 | 33.56 | 37.30 | 34.66 | 33.02 | 33.12 | 33.21 | 33.68 | 33.68 | 35.92 | 36.12 | 36.12 | 37.11 |
| 21–22 | 34.88 | 33.21 | 34.04 | 36.29 | 34.28 | 33.58 | 33.64 | 33.54 | 33.70 | 33.70 | 36.75 | 37.08 | 37.08 | 37.08 |
| 22–23 | 33.84 | 32.80 | 33.46 | 35.02 | 34.00 | 33.56 | 33.60 | 33.14 | 33.66 | 33.66 | 34.30 | 34.30 | 34.30 | 37.13 |
| 23–24 | 32.55 | 32.14 | 32.57 | 32.83 | 32.84 | 32.82 | 32.84 | 30.97 | 32.93 | 30.97 | 30.97 | 30.97 | 30.97 | 34.23 |

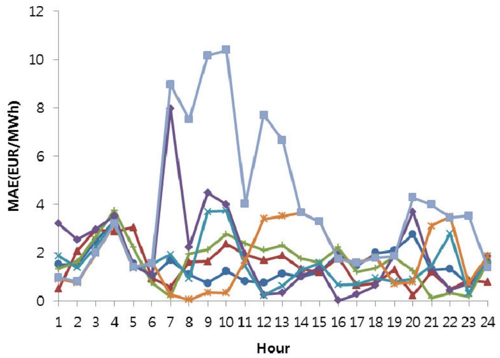


**Fig. 3.** Hourly MAE (EUR/MWh) for the test periods in the Nord Pool

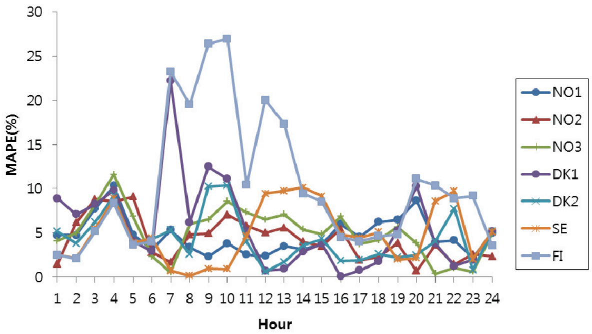


**Fig. 4.** Hourly MAPE (%) for the test periods in the Nord Pool

**Table 3.** Statistical analysis of forecasting error

| Area | MAE (EUR/MWh) | RMSE (EUR/MWh) | Error variance ( $\sigma^2$ ) |
|---|---|---|---|
| NO1 | 1.51 | 1.64 | 9.23911E-05 |
| NO2 | 1.45 | 1.65 | 2.87827E-07 |
| NO3 | 1.65 | 1.87 | 9.65566E-05 |
| DK1 | 2.05 | 2.71 | 8.23861E-05 |
| DK2 | 1.57 | 1.84 | 9.87736E-06 |
| SE | 1.76 | 2.11 | 2.39391E-05 |
| FI | 3.99 | 4.94 | 0.000304247 |

the purpose of evaluating out of forecasting capability. The first column indicates the bidding area of Nord Pool, the second column presents the MAE (EUR/MWh), the third column presents the RMSE (EUR/MWh), and the fourth column presents the error variance ( $\sigma^2$ ). The MAE and RMSE of reasonably small values were obtained for the Nord Pool data. The error variance, one of the important performance criteria, is also calculated in order to measure robustness of the proposed approach. The smaller the variance, the more precise is the prediction of LMPs. As shown in Table 3, small value of $\sigma^2$ was obtained for the test periods in the Nord Pool.

Fig. 5 shows a comparison between the proposed approach and the time-series techniques, in what regards the MAPE criterion. The results obtained shows that the proposed forecast strategy is better for NO1, NO3, DK1, DK2, SE, and FI than the ARIMA and GARCH for all the

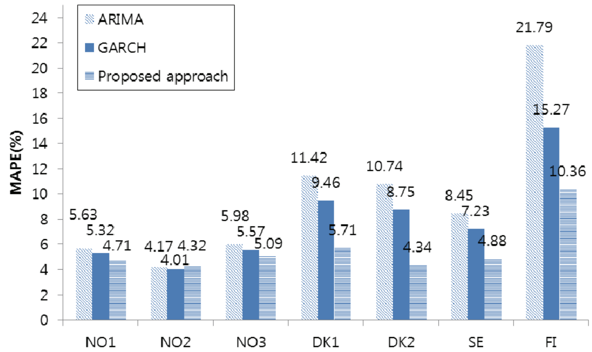


**Fig 5.** Comparative MAPE (%) results

test periods due to its forecasting engine. Furthermore, because the proposed forecasting strategy had lower error variances, its predictions were more stable. During the peak hours, the volatility of the Nord Pool increased, and so time-series techniques had considerably larger prediction errors, but when the variance of the data is more stable, as was the case for NO2, then the price volatility was less accurate. Although some promising results have been obtained from time-series techniques for LMP prediction, most of these methods are linear techniques and cannot appropriately track the complex non-linear behavior of LMP signals. Ultimately, the time-series techniques may encounter large unexpected forecasting errors. Rapid variations and high-frequency changes in the target signal are problematic for the time-series techniques. However, because of the ANN's capability of tracking non-linear behavior in the price signal, it is preferred in practical applications. Consequently, the proposed approach has high forecasting accuracy and its performance is less affected by volatility, which can be of the utmost importance in real-life applications.

## 5. Conclusions

Accurate forecasting approach is essential not only for producers to maximize their profits, but also for consumers to maximize their utilities. This paper proposed a new prediction strategy for short-term electricity price forecasting. In this work, the ANN technique was applied to forecast the LMPs. A three-layered feed-forward neural network model, trained using the LM algorithm, is particularly suited for the short-term forecasting, implementing nonlinearities using sigmoid functions for the hidden layer and linear functions for the output layer. To increase the accuracy of our predictions, actual power generation and load were considered as the input sets, based on historical data. After forecasting each area of power generation and load, these differences can be generalized for analyzing the causes of price differences in the spot market. The LMP calculation is iterated so that the trading capacity between the areas is used to the maximum, to ensure that energy flows from the low-price area towards the high-price area. Thus, the LMPs in the surplus and deficit areas are found as the new equilibrium points after the addition of power flow between the areas for purchase and sale, respectively. The simulation results not only revealed the forecasting capabilities of the proposed strategy, but also demonstrated its forecasting accuracy. Moreover, the proposed forecasting strategy was compared with the time-series techniques. The MAPE results from the comparisons clearly showed that the proposed approach was more effective than the time-series techniques. Especially for peak hours, ARIMA demonstrated considerably larger prediction errors because of, high volatility, price spikes, and nonlinear behavior of LMP signal while the proposed approach showed relatively accurate predictions. Therefore, the application of the proposed approach to price forecasting is both novel and effective. The research work is under way in order to develop better feature selection in this field of study, because of nonlinear behavior of electricity price signal.

## Appendix

The description of two models based on time-series analysis is presented to forecast the electricity price: ARIMA and GARCH. It is assumed that price values are recorded at fixed time intervals.

### A.1 ARIMA

If $p_t$ denotes the electricity price at time $t$, the ARIMA formulation has the following form [17]:

$$\phi(B)p_t = \theta(B)\varepsilon_t \tag{A.1}$$

where $\phi(B)$ and $\theta(B)$ are functions of the backshift operator $B : B^l p_t = p_{t-l}$ , and $\varepsilon_t$ is the error term. Functions $\phi(B)$ and $\theta(B)$ have special forms. They can contain factors of polynomial functions of the form $\phi(B)=1-\sum^{\Phi}_{l=1}\phi_l B^l$, and/or $\theta(B)=1-\sum^{\Theta}_{l=1}\theta_l B^l$, and/or $(1-B^S)$, where several values of $\phi_l$ and $\theta_l$ can be set to 0.

In an ARIMA(p, q, d), p stands for the order of the autoregressive process, q is the order of the moving average process, and d represents the degree of differencing involved. The detail information can be found in [17].

### A.2 GARCH

The general GARCH model has the form given below [20]:

$$h_t = c + \sum_{i=1}^{p} \alpha_i h_{i-1} + \sum_{i=1}^{q} \beta_i \varepsilon_{t-i}^2 \tag{A.2}$$

where $\varepsilon_t$ is a white noise, and $\varepsilon_t^2$ takes the form

$$\varepsilon_t^2 = v_t^2 h_t \tag{A.3}$$

Here, $\varepsilon_t$ is GARCH(1,3) model, as it incorporates mean reversion, the dynamics of $\varepsilon_t^2$ can be explained through past volatility shocks $\varepsilon_{t-i}^2$.

### A.3 Procedure of time series models

The process of two models is based on three steps: (1) model identification, (2) parameter estimation, and (3) diagnostic checking. In the first step, an initial model is built, hypotheses are established, and an initial selection of parameters is based on the observation of the autocorrelation and partial autocorrelation plots. In the second step, the optimal parameters are determined by the use of maximizing a likelihood function for the available data. In the third step, this step is done by plotting the model residuals. If the estimated model is appropriate, then, the residuals (actual prices minus predicted prices) should behave in a manner consistent with the model. As a result of these three steps, the final models for the Nord Pool are described in (A.4).

$$\begin{aligned}
&(1-\varphi_1 L^1 - \varphi_2 L^2 - \varphi_3 L^3 - \varphi_4 L^4 \\
&-\varphi_{23} L^{23} - \varphi_{24} L^{24} - \varphi_{25} L^{25} - \varphi_{47} L^{47} \\
&-\varphi_{48} L^{48} - \varphi_{49} L^{49} - \varphi_{167} L^{167} - \varphi_{168} L^{168} \\
&-\varphi_{169} L^{169} - \varphi_{335} L^{335} - \varphi_{336} L^{336} - \varphi_{337} L^{337} \\
&-\varphi_{503} L^{503} - \varphi_{504} L^{504} - \varphi_{505} L^{505} - \varphi_{671} L^{671} \\
&-\varphi_{672} L^{672} - \varphi_{673} L^{673}) \cdot \log(p_t) = c + \varepsilon_t
\end{aligned} \tag{A.4}$$

## Acknowledgements

This Research was supported by the Chung-Ang University Research Grants in 2014.

## References

[1] M. A. F. Ghazvini, B. Canizes, Z. Vale and H. Morais, “Stochastic short-term maintenance scheduling of GENCOs in an oligopolistic electricity market,” *Appl Energy*, vol. 101, no. 1, pp. 667-677, Jan. 2013.

[2] M. Shahidehpour, H. Yamin and Z. Li, *Market operations in electric power systems*: John Wiley & Sons, Inc., Publication, 2002

[3] Gong Li and Jing Shi, “Agent-based modeling for trading wind power with uncertainty in the day-ahead wholesale electricity markets of single-sided auctions,” *Appl Energy*, vol. 99, no. 1, pp. 13-22, Nov. 2012.

[4] D. W. Bunn, “Forecasting loads and prices in competitive power markets,” *in Proceedings of IEEE*, vol.

88, no. 2, pp. 163-69, Feb. 2000.

[5] J. Wang, S. Zhu, W. Zhang and H. Lu, "Combined modeling for electric load forecasting with adaptive particle swarm optimization," *Energy*, vol. 35, no. 4, pp. 1671-1678, Apr. 2010.

[6] M.R. AlRashidi and K.M. EL-Naggar, "Long term electric load forecasting based on particle swarm optimization," *Appl Energy*, vol. 87, no. 1, pp. 320-326, Jan. 2010.

[7] J. Wang, L. Li, D. Niu and Z. Tan, "An annual load forecasting model based on support vector regression with differential evolution algorithm," *Appl Energy*, vol. 94, pp. 65-70, Jun. 2012.

[8] C. Wang, G. Grozev and S. Seo, "Decomposition and statistical analysis for regional electricity demand forecasting," *Energy*, vol. 41, no. 1, pp. 313-325, May. 2012.

[9] R. Deb, R. Albert, L. L. Hsue and N. Brown, "How to incorporate volatility and risk in electricity price forecasting," *Electricity J*, pp. 1-16, May. 2000.

[10] D. J. Pedregal and J. R. Trapero, "Mid-term hourly electricity forecasting based on a multi-rate approach," Energy Convers Manage, vol. 51, no. 1, pp. 105-111, Jan. 2010.

[11] M. K. Kim, Y. W. Nam and J. K. Park, "Market-clearing for pricing system security based on voltage stability criteria," *Energy*, vol. 36, no. 2, pp. 1255-1264, Feb. 2011.

[12] E. Ni and P. B. Luh, "Forecasting power market clearing price and its discrete PDF using a Bayesian-based classification method," *IEEE Power Eng. Soc. Winter Meeting 2001*, Columbus, Jan. 2001.

[13] L. Zhang and P. B. Luh, "Neural network-based market clearing price prediction and confidence interval estimation with an improved extended Kalman filter method," *IEEE Trans Power Syst*, vol. 20, no. 1, pp. 59-66, Feb. 2005.

[14] M. K. Kim and D. Hur, "An optimal pricing scheme in electricity markets by parallelizing security constrained optimal power flow based market-clearing model," *Int J Electr Power Energy Syst*, vol. 48, pp. 161-171, Jun. 2013.

[15] C. P. Rodriguez and G. J. Anders, "Energy price forecasting in the Ontario competitive power system market," *IEEE Trans Power Syst*, vol. 19, pp. 366-374, Feb. 2004.

[16] F. J. Nogales, J. Contreras, A. J. Conejo and R. Espinola, "Forecasting next-day electricity prices by time series models," *IEEE Trans Power Syst*, vol. 17, no. 2, pp. 342-348, May. 2002.

[17] J. Contreras, R. Espinola, F. J. Nogales and A. J. Conejo, "ARIMA models to predict next day electricity prices," *IEEE Trans Power Syst*, vol. 18, no. 3, pp. 1014-1020, Aug. 2003.

[18] A. J. Conejo, M. A. Plazas, R. Espinola and A. B. Molina, "Day-ahead electricity price forecasting using the wavelet transform and ARIMA models," *IEEE Trans Power Syst*, vol. 20, pp. 1035-1042, May. 2005.

[19] Z. Tan, J. Zhang, J. Wang and J. Xu, "Day-ahead electricity price forecasting using wavelet transform combined with ARIMA and GARCH models," *Appl Energy*, vol. 87, no. 11, pp. 3606-3610, May. 2010.

[20] R. Garcia, J. Contreras, M. van Akkeren and J. Garcia , "A garch forecasting model to predict day-ahead electricity prices," Power Systems, *IEEE Trans Power Syst*, vol. 20, no. 2, pp. 867-874, May. 2005.

[21] B. R. Szkuta, L. A. Sanabria and T. S. Dillon, "Electricity price short-term forecasting using artificial neural networks," *IEEE Trans Power Syst*, vol. 14, no. 3, pp. 851-858, Aug. 1999.

[22] S. A. Kalogirou, "Applications of artificial neural-networks for energy systems," *Appl Energy*, vol. 67, no. 1, pp. 17-35, Sept. 2000.

[23] L. Zhang, P. B. Luh and K. Kasivisvanathan, "Energy clearing price prediction and confidence interval estimation with cascaded neural networks," *IEEE Trans Power Syst*, vol. 18, no. 1, pp. 99-105, Feb. 2003.

[24] H. Y. Yamin, S. M. Shahidehpour and Z. Li, "Adaptive short-term electricity price forecasting using artificial neural networks in the restructured power markets," *Int J Electr Power Energy Syst*, vol. 26, pp. 571-581, Oct. 2004.

[25] M. P. Garcia and D. S. Kirschen, "Forecasting system imbalance volumes in competitive electricity markets," *IEEE Trans Power Syst*, vol. 21, pp. 240-248, Feb. 2006.

[26] S. K. Aggarwal, L. M. Saini and A. Kumar, "Electricity price forecasting in deregulated markets: a review and evaluation," *Int J Electr Power Energy Syst*, vol. 31, no.1, pp. 13-22, Jan. 2009.

[27] R. Gareta, L. M. Romeo and A. Gil, "Forecasting of electricity prices with neural networks," *Energy Convers Manage*, vol. 47, pp. 1770-1778, Aug. 2006.

[28] H. T. Nguyen and I. T. Nabney, "Short-term electricity demand and gas price forecasts using wavelet transforms and adaptive models," *Energy*, vol. 35, no. 9, pp. 3674-3685, Jan. 2010.

[29] W. M. Lin, H. J. Gow and M. T. Tsai, "An enhanced radial basis function network for short-term electricity price forecasting," *Appl Energy*, vol. 10, pp. 3226-3234, Oct, 2010.

[30] P. Mandal, T. Senjyu, N. Urasaki and T. Funabashi, "A neural network based several hour-ahead electric load forecasting using similar days approach," *Int J Electr Power Energy Syst*, vol. 28, pp. 367-373, Jul. 2006.

[31] Y. Y. Hong and C. Y. Hsiao, "Locational marginal price forecasting in deregulated electricity markets using artificial intelligence" *IEE Proc Generation Trans Distribution*, vol. 149, no. 5, pp. 621-626, Sept. 2002.

[32] X. Lu, Z. Y. Dong and X. Li, "Electricity market price spike forecast with data mining techniques," *Electric Power Syst Res*, vol. 73, pp. 19-29, Jan. 2005.
[33] J. H. Zhao, Z. Y. Dong, X. Li and K. P. Wong. "A general method for electricity market price spike analysis. In," *IEEE Power Eng. Soc. General Meeting, IEEE 2005*, vol. 1, pp. 1286-1293, Jun. 2005.
[34] S. Haykin, *Neural Networks: A Comprehensive Foundation*: New York, Macmillan, 1994.
[35] N. Amjady and F. Keynia, "A new spinning reserve requirement forecast method for deregulated electricity markets," *Appl Energy*, vol. 87, no. 6, pp. 1870-1879, Jun. 2010.
[36] M. H. Khosravi, S. Barghinia and P. Ansarimehr, "New momentum adjustment technique for Levenberg-Marquardt neural network training used in short term load forecasting", *Int Power Syst Conference*, pp. 1782-1788, 2006.
[37] M. K. Kim and D. Hur, "Decomposition-coordination strategy to improve power transfer capability of inter-connected systems," *Int J Electr Power Energy Syst*, vol. 33, no. 10, pp. 1638-1647, 2011.
[38] Nord Pool spot market. [Online]. Available: <http://www.nordpoolspot.com/>.
[39] The MathWorks, MATLAB. [Online]. Available: <http://www.mathworks.com>.

**Mun-Kyeom Kim** was born in Korea, on 1976. He received B.S. degree in Electrical Engineering from Korea University, Seoul, Korea in 2004 and M.S. and Ph.D. degrees in Electrical Engineering from Seoul National University, Seoul, Korea in 2006 and 2010, respectively. He worked as a post-doc in the institute of information technology in the department of electrical engineering at Seoul National University. He is currently an assistant professor in the Department of Energy System Engineering, Chung-Ang University, Seoul, Korea. His research interests include the intelligent power network, HVDC, wind power and the real-time market design in smart grid.